HHS Public Access

Author manuscript

Sci Transl Med. Author manuscript; available in PMC 2019 April 02.

Published in final edited form as:

Sci Transl Med. 2018 November 14; 10(467): . doi:10.1126/scitranslmed.aat4271.

Commensal bacteria contribute to insulin resistance in aging by activating innate B1a cells

Monica Bodogai[1], **Jennifer O'Connell**[2], **Ki Kim**[1], **Yoo Kim**[2], **Kanako Moritoh**[1], **Chen Chen**[1], **Fedor Gusev**[3], **Kelli Vaughan**[4], **Natalia Shulzhenko**[5], **Julie A. Mattison**[4], **Catalina Lee-Chang**[16], **Weixuan Chen**[7], **Olga Carlson**[2], **Kevin G. Becker**[8], **Manoj Gurung**[5], **Andrey Morgun**[9], **James White**[10], **Theresa Meade**[11], **Kathy Perdue**[11], **Matthias Mack**[12], **Luigi Ferrucci**[13], **Giorgio Trinchieri**[14], **Rafael de Cabo**[13], **Evgeny Rogaev**[3,15,16], **Josephine Egan**[2], **Jiejun Wu**[7], and **Arya Biragyn**[1,*]

[1]Immunoregulation Section, National Institute on Aging, Baltimore, MD 21224, USA.

[2]Laboratory of Clinical Investigation, National Institute on Aging, Baltimore, MD 21224, USA.

[3]Department of Genomics and Human Genetics, Vavilov Institute of General Genetics, Russian Academy of Sciences, Moscow, Russia.

[4]Nonhuman Primate Core Facility, National Institute on Aging, Baltimore, MD 21224, USA.

[5]College of Veterinary Medicine, Oregon State University, Corvallis, OR 97331, USA.

[6]Department of Neurological Surgery, Brain Tumor Research Institute, The Feinberg School of Medicine, Northwestern University, Chicago, IL 60611, USA.

[7]Janssen Research & Development, San Diego, CA 92121, USA.

[8]Laboratory of Genetics, National Institute on Aging, Baltimore, MD 21224, USA.

[9]College of Pharmacy, Oregon State University, Corvallis, OR 97331, USA.

[10]Resphera Biosciences, Baltimore, MD 21231, USA.

[11]Comparative Medicine Section, National Institute on Aging, Baltimore, MD 21224, USA.

[12]Department of Nephrology, Universitätsklinikum Regensburg, Regensburg 93001-93059, Germany.

[13]Longitudinal Studies Section, Translational Gerontology Branch, National Institute on Aging, Baltimore, MD 21224, USA..

[14]Cancer Inflammation Program, National Cancer Institute, Frederick, MD 21701, USA.

*Corresponding author. biragyna@mail.nih.gov.

Author contributions: M.B. designed and performed the research and collected and analyzed data; K.K., J.O., K.M., K.V., C.L.-C., C.C., Y.K., W.C., J. Wu, and O.C. performed experiments; N.S., A.M., M.G., M.M., T.M., and K.P. contributed to vital new reagents; J.A.M., F.G., K.G.B., J. White, G.T., L.F., R.d.C., E.R., J.E., and J. Wu provided critical interpretation; and A.B. wrote the manuscript and conceived, designed, and supervised the study.

Competing interests: The authors declare that they have no competing interests.

Data and materials availability: All data associated with this study can be found in the paper or the Supplementary Materials. Raw data are provided in table S3. 4–1BBL KO mice are available upon completion of a material transfer agreement. Anti-CCR2 Ab is from Matthias.Mack@klinik.uni-regensburg.de

[15]Center for Genetics and Genetic Technologies, Faculty of Biology, Faculty of Bioengineering and Bioinformatics, Lomonosov Moscow State University, Moscow, Russia.

[16]Brudnick Neuropsychiatric Research Institute, University of Massachusetts Medical School, Worcester, MA 01604, USA..

Abstract

Aging in humans is associated with increased hyperglycemia and insulin resistance (collectively termed IR) and dysregulation of the immune system. However, the causative factors underlying their association remain unknown. Here, using "healthy" aged mice and macaques, we found that IR was induced by activated innate 4–1BBL^{+} $_{\text{B1a cells.}}$ These cells (also known as 4BL cells) accumulated in aging in response to changes in gut commensals and a decrease in beneficial metabolites such as butyrate. We found evidence suggesting that loss of the commensal bacterium *Akkermansia muciniphila* impaired intestinal integrity, causing leakage of bacterial products such as endotoxin, which activated CCR2^{+} monocytes when butyrate was decreased. Upon infiltration into the omentum, CCR2^{+} monocytes converted B1a cells into 4BL cells, which, in turn, induced IR by expressing 4–1BBL, presumably to trigger 4–1BB receptor signaling as in obesity-induced metabolic disorders. This pathway and IR were reversible, as supplementation with either *A. muciniphila* or the antibiotic enrofloxacin, which increased the abundance of *A. muciniphila*, restored normal insulin response in aged mice and macaques. In addition, treatment with butyrate or antibodies that depleted CCR2^{+} monocytes or 4BL cells had the same effect on IR. These results underscore the pathological function of B1a cells and suggest that the microbiome–monocyte–B cell axis could potentially be targeted to reverse age-associated IR.

INTRODUCTION

Aging is associated with chronic inflammation, a hallmark of and a risk factor for the development of age-associated pathologies such as hyperglycemia and insulin resistance (collectively termed IR) (1). Although the cause of chronic inflammation remains poorly understood, an emerging concept implicates gut microbiota (2) whose compositional change can lead to gut leakiness and subsequent activation of innate immune responses (3). The ratio of proinflammatory to beneficial commensals can become increased in the fecal microbial community of the elderly and particularly in frail individuals (4–6). In recent independent studies of Italian centenarians (4) and long- living Chinese individuals (5), longevity inversely correlated with the alpha diversity of fecal microbiota and positively associated with the abundance of beneficial commensals (such as *Clostridium* cluster *XIVa*, *Ruminococcaceae*, and *Akkermansia*) that metabolize fibers into short- chain fatty acids (SCFAs; such as acetate, propionate, and butyrate). The reduction of SCFAs can lead to loss of intestinal integrity (7) because it provides energy and induces oxygen consumption of colonocytes (8). As an inhibitor of Toll-like receptor 4 (TLR4) signaling (9) and histone deacetylases (10), a decrease in butyrate in the intestine also allows microbes and microbial products to efficiently activate the production of proinflammatory cytokines and chemokines in myeloid cells (11). *Akkermansia muciniphila* is a Gram-negative anaerobic bacterium that induces the mucin production necessary for intestinal integrity and potentially for the support of other beneficial commensals. Its predicted outer membrane protein Amuc_1100*

has been shown to improve gut barrier function and metabolic endotoxemia in mice with diet-induced obesity by stimulating TLR2 (12). Correspondingly, the loss of *A. muciniphila* associates with poor fitness and increased frailty due to gut dysbiosis and leakiness, which ultimately results in endotoxemia and a mild proinflammatory state with elevated levels of interferons (IFNs), tumor necrosis factor–α (TNFα), interleukin-6 (IL-6), and IL-1 (4–6, 13, 14).

The immune system is also substantially dysregulated in aging. Bone marrow hematopoiesis becomes skewed to myelopoiesis (15), and peripheral sites accumulate activated innate immune cells including monocytes and macrophages expressing TNFα and IFN-γ (13, 14). Reduced bone marrow lymphopoiesis and lifelong antigenic exposure increase the frequency of mature and memory lymphocytes (16), which exhibit exhausted and overactivated phenotypes, such as aging-associated B cells in mice (17, 18) and highly differentiated $CD45RA^{+}CD8^{+}$ $CD28^{-}$ T cells in humans (16). We previously reported that aged humans, primates, and mice accumulate innate B1a B cells expressing 4–1BBL, TNFα, and major histocompatibility complex class I cells (termed 4BL cells) by using an unknown subset of $CD11b^{+}$ phagocytic mononuclear cells that express 4–1BB, CD40, and IFN-γ (19, 20). However, although 4BL cells induce the generation of potentially autoimmune granzyme $(GrB)^{+}$ $CD8^{+}$ T cells (19, 20), the clinical relevance of these findings and the nature of the inducer myeloid cells remain unknown.

Here, to understand the IR increase in elderly humans and the accumulation of 4BL cells in aging, we sought to determine whether the two could be linked by a common cause, the gut microbiota. Because 4BL cells highly express 4–1BBL and TNFα, factors implicated in obesity-induced adipose inflammation and metabolic disorders (21), we hypothesized that 4BL cells induced IR in aging. We found that a reduction of beneficial commensal gut microbiota and their metabolites, such as butyrate, induced the generation of 4BL cells, which subsequently promoted IR in aged mice and macaques. Mechanistically, the process was initiated by the loss of *A. muciniphila*, resulting in gut leakiness in aged mice. When butyrate was reduced in the gut and subsequently in the peritoneal cavity (PeC), the leaked microbial inflammatory stimuli activated $CCR2^{+}$ monocytes, which, upon infiltration into the omentum, converted B1a cells into 4BL cells. This resulted in impaired insulin signaling in peripheral tissues. Overall, we link IR in aging to 4BL cells and show that this pathology is reversible in mice and macaques, as it can be eliminated by targeting the upstream factors that cause 4BL cell induction.

RESULTS

Monocytes in aging mice induce 4BL cells

We previously reported that the conversion of B1a cells into 4BL cells in the PeC of aged mice is mediated by granulocyte-depleted phagocytic $CD11b^{+}$ myeloid cells (20). Because myeloid cells consist of macrophages ($CD11c^{-}F4/80^{Hi}CD11b^{Hi}$), dendritic cells ($F4/80^{-}CD11C^{+}CD11b^{+}$), and monocytes ($F4/80^{-/Lo}$ $CD11C^{-/Lo}Ly6C^{+}CD11b^{+}$, which mostly comprise bone marrow–derived $CCR2^{+}Ly6C^{Hi}$ monocytes and early- activated monocyte-derived macrophages (22), we used flow cytometry to analyze these cells in the PeC of 8- to 20-week-old and 18- to 24-month-old female C57BL/6 mice (respectively

designated young and aged mice; fig. S1A). Compared with young mice, aged mice were markedly enriched in monocytes and dendritic cells and depleted in macrophages (in terms of both numbers and frequency; Fig. 1, A to D, and fig. S1, B to E). In particular, aged mice had increased monocytes expressing CCR2 (Fig. 1E), and all three factors known to induce 4BL cells (IFN-γ, 4–1BB, and CD40L; Fig. 1, F to H) (19, 20). In contrast, dendritic cells only moderately expressed 4–1BB and CD40L, whereas macrophages did not express any of these factors (fig. S1, F and G). Compared to dendritic cells and macrophages, only monocytes profoundly up-regulated expression of 4–1BB and other inflammation-associated genes in aging (Fig. 1I and fig. S1, H and I). Also, in an in vitro 4BL cell conversion assay (20), only monocytes, but not dendritic cells and macrophages, induced the expression of 4–1BBL and mTNFα in B1a cells after overnight coculture (Fig. 1, J to L). Hence, by accumulating activated monocytes, aging converted B1a cells into 4BL cells.

The conversion of B1a to 4BL cells occurs in the omentum

Compared with young mice, CCL2 and CXCL13 were markedly increased in the PeC lavage of aged mice (fig. S2A). Because these chemokines recruit $CCR2^+$ myeloid cells and B1a cells in inflamed and aged omentum (23, 24), we tested whether this is the site of the 4BL cell conversion. Quantification of $4–1BBL^+$ B cells in multiple sites where B1 cells infiltrate, such as omentum, Peyer's patches, and mesenteric lymph nodes (25–27), revealed that only aged omentum was predominantly enriched in $4–1BBL^+$ B1a cells (Fig. 2A and fig. S2, B to D). Monocytes were also increased in omentum (fig. S2E) and were colocalized with B cells and, importantly, with $4–1BBL^+$ B cells in whole-mount immunofluorescence staining (Fig. 2B). To further validate this result, we transferred bone marrow $CD45.1^+$ monocytes and PeC green fluorescent protein–positive (GFP^+) B1 cells of young mice into $CD45.2^+$ young or aged mice via tail vein injection. After 2 days, higher numbers of donor monocytes and B1 cells were found in aged omentum and PeC as compared with young mice (fig. S2, F and G). To test whether this increase facilitated the 4BL cell conversion, we in vitro stimulated $eFluor450^+$ B1 cells from young mice with omentum isolated from either young or aged mice. After overnight coculture, only aged omentum up-regulated 4–1BBL in $eFluor450^+$ B1 cells (Fig. 2C). To link the 4BL cell conversion to $CCR2^+$ monocytes, we treated aged mice with either MC21 antibody (Ab), which depletes $CCR2^+$ monocytes (28), or control MC67 Ab for 10 to 14 days. Mice were then adoptively transferred with GFP^+ B1a cells from young mice, and 6 days later, host and donor cells were quantified. As expected, host 4BL cells and monocytes (Fig. 2D and fig. S2H) and donor $4–1BBL^+$ GFP^+ B1a cells were markedly increased in the omentum and PeC of control mice (Fig. 2E). However, this increase of host and donor cells was markedly reversed in aged mice treated with MC21 Ab (Fig. 2, D and E, and fig. S2H). In sum, these results indicate that aging omentum may be the site where $CCR2^+$ monocytes convert B1a cells into 4BL cells.

Commensal bacteria in aged mice initiate 4BL cell conversion

The PeC lavage of aged mice also contained high concentrations of inflammatory factors such as lipocalin (fig. S2A). As lipocalin is often induced by bacterial gut leakage (29), we hypothesized that commensal bacteria may initiate 4BL cell induction in aged mice. To test this possibility, we treated young and aged mice with enrofloxacin [a broad-spectrum antibiotic (Abx)] in drinking water for 16 weeks. The accumulation of monocytes, 4BL

cells, and their downstream GrB^+CD8^+ T cells in PeC and omentum in control saline-treated aged mice was abolished in the Abx-treated aged mice (Fig. 3, A to E). We repeated the experiment, and then 2 days after cessation of Abx treatment, mice were transferred with GFP^+ B1 cells from young mice. Consistent with the loss of monocytes (Fig. 3D), the 4BL cell conversion of donor GFP^+ B1 cells was abolished in the aged mice treated with Abx (Fig. 3F and fig. S2I). To confirm this result, we performed an in vitro 4BL conversion assay by stimulating splenic or PeC $eFluor450^+$ B1a cells from young mice overnight with PeC Lin^-CD11b^+ myeloid cells from young or aged mice previously treated with water or Abx. Although myeloid cells from aged mice efficiently converted 4BL cells, myeloid cells from Abx-treated aged mice or young mice failed to do so (Fig. 3G and fig. S2J). Hence, Abx impairs the generation of 4BL cells in a monocyte-dependent fashion.

Consistent with the accumulation of 4BL cells in aging humans and primates (19, 20), we observed that the peripheral blood of aged macaques and squirrel monkeys was markedly enriched in 4BL cells (fig. S3, A and B), suggesting that this enrichment might also be reversible by Abx. We therefore treated aged macaques with enrofloxacin for 2 months (n = 7 to 8 per group). Abx treatment decreased 4BL and GrB^+CD8^+ T cells (Fig. 3H and fig. S3C). To link this result to monocytes, young macaque peripheral blood B cells were stimulated overnight with peripheral blood monocytes from young, aged, or Abx-treated aged macaques. Only monocytes from aged, but not Abx-treated aged or young macaques, readily converted 4BL cells (Fig. 3I). In sum, enrofloxacin abrogated monocyte-mediated 4BL cell conversion in aged mice and primates, presumably by eliminating their inducer bacteria.

Aging increases microbial dysbiosis

Because gut microbiota dysbiosis can increase in aging (2, 3), we tested whether dysbiosis caused the 4BL cell conversion. First, we performed cross-sectional 16*S* ribosomal RNA (rRNA) gene sequencing of fecal microbiota from young and aged mice after 3 months of mock or Abx treatment. Microbial communities of aged and young mice differed markedly ($P \leq 1 \times 10^{-3}$ for all group comparisons; fig. S4, A to C). Compared to young mice, microbiota alpha diversity was reduced in aged and Abx-treated groups (fig. S4D), and aged mice were markedly enriched in the proinflammatory phylum Firmicutes and decreased in the genus *Bacteroides* (fig. S4, E and F). Aged mice also had an increased abundance of the genera *Parabacteroides* and *Saccharofermentans*, as well as unassigned genera within the family *Lachnospiraceae* (Fig. 4A). Furthermore, aged mice showed reduced potentially beneficial commensals, including *A. muciniphila* (30) and butyrate producers of the Firmicutes phylum (31–33) such as *Intestinimonas butyriciproducens*, *Faecalibacterium prausnitzii* and *Roseburia faecis* of *Clostridium* cluster *IV*, and *Anaerostipes butyraticus* of *Clostridium* cluster *XIVa* (Fig. 4A, fig. S4F, and table S1). Because these results can be affected by external factors, we sequenced fecal microbiota from additional C57BL/6 mice purchased from two different vendors (the Jackson Laboratory and Charles River Laboratories). Compared to young mice, *A. muciniphila* and *Clostridium* cluster *IV* were again reduced in both cohorts of aged mice (fig. S4, G and H). The abundance of *A. muciniphila* (herein denoted as Akk) inversely correlated with 4BL cells in both PeC and spleen (Fig. 4B and fig. S5A).

To evaluate the functional consequence of this change, we gavaged adult germ-free mice with fecal suspensions from aged or young mice housed in a standard pathogen-free (SPF) facility. After 1 month, quantitative polymerase chain reaction (qPCR) analysis confirmed that the gavaged mice were successfully colonized (fig. S5B). Fecal suspensions from both aged and young mice showed comparably induced IL-10^+ and IL-17^+ $CD4^+$ T cells in the germ-free mice (fig. S5, C and D), implying that their induction is independent of the age of the microbiota's host. In contrast, only fecal suspension from aged mice increased 4BL cells and monocytes in the omentum/PeC of germ- free mice (Fig. 4C and fig. S5E), implying that aging gut microbiota causes the 4BL cell conversion.

The loss of Akk increases gut leakiness and induces 4BL cells

The 4BL cell increase in germ-free mice after fecal transfer inversely associated with the acquisition of Akk as in parental SPF mice. qPCR and sequencing analyses failed to detect Akk in germ-free mice transplanted with fecal suspension from aged mice, whereas Akk was increased in mice gavaged with feces from young mice (fig. S5B, F and G). Because Akk protects the intestinal integrity via mucus support and activation of intestinal epithelial cells (12, 30, 34), its reduction in aging is expected to increase gut leakiness and thus the inflammation that activates monocytes. To test this possibility, we compared the intestinal mucus layer in young and aged SPF mice and found that the colonic inner mucus width was decreased in aged mice (Fig. 4D). To directly test gut leakage, we orally gavaged aged and young mice with fluorescein isothiocyanate–dextran (FITC-dextran; 3 to 5 kDa). After 4 hours, FITC-dextran was increased in the plasma of aged compared to young mice (Fig. 4E), consistent with impaired intestinal permeability in murine aging (35). We also measured serum endotoxin and confirmed that it was increased in the sera of aged mice (Fig. 4F). There was no difference in serum endotoxin of germ-free mice gavaged with fecal suspension from aged and young SPF mice (fig. S5H). To link gut leakiness to the loss of Akk, we gavaged aged mice with either sterile saline or Akk for 20 days (fig. S5I) and then orally gavaged with FITC-dextran. The decreased colonic inner mucus and increased FITC-dextran and endotoxin leakage in aged mice were reversed in Akk-treated aged mice, almost to that observed in young mice (Fig. 4, D to F). The Akk treatment also completely abolished the enrichment of 4BL cells and their downstream GrB^+CD8^+ T cells (Fig. 4, G and H, and fig. S5J). Because enrofloxacin increased Akk (Fig. 4A), presumably due to Abx resistance (36), and eliminated 4BL cells in aged mice, we reasoned enrofloxacin might also be able to reverse gut leakage. To test this possibility, we measured the presence of functionally active endotoxin in sera of mock- and enrofloxacin-treated mice using nuclear factor κB reporter HEK-Blue-4 cells stably expressing human *TLR4* and its coreceptor genes *MD-2* and *CD14*. Abx reversed the increased serum endotoxin (Fig. 4I) and leakage of orally administered FITC-dextran (Fig. 4J) in aged mice back to concentrations seen in young mice. Together, these results indicate that Akk prevented the generation of 4BL cells, at least in part, by protecting the intestinal epithelial integrity.

Butyrate controls the induction of 4BL cells

Because of its importance for some commensals (30, 37), the decrease in the mucus layer in aging could explain the reduction of bacteria in *Clostridium* clusters *IV* and *XIVa*, such as *I. butyriciproducens*, *F. prausnitzii*, *R. faecis*, and *A. butyraticus*. Because these bacteria

metabolize fiber into immunoregulatory SCFAs (7), we hypothesized that their loss increases inflammation, thereby activating monocytes to induce 4BL cells. First, we quantified SCFA in various regions of the intestine, PeC lavage, and feces of mice and macaques using liquid chromatography–mass spectrometry (fig. S6, A and B). Compared to young, aged mouse intestine (particularly cecum; Fig. 5A and fig. S6C) and the feces of elderly macaques (fig. S6D) were markedly reduced in acetate, propionate, and butyrate. In PeC lavage, however, only butyrate was decreased in aged mice (Fig. 5B and fig. S6C). Because butyrate inhibits lipopolysaccharide (LPS)–induced monocyte inflammation (38), we sought to determine whether its decrease in PeC enabled activation of monocytes by microbial stimuli (such as LPS) leaked from guts of aged mice. First, we artificially increased the LPS concentration in PeC of young mice by intraperitoneally injecting a low dose of LPS (5 μg) daily for 5 days. We observed an increase in monocytes (IFN-γ^+4–1BB$^+$CD40L$^+$) and 4BL cells in the omentum/PeC (fig. S7, A to H). To confirm this result in vitro, bone marrow–derived monocytes from naïve young mice were stimulated overnight with LPS (100 ng/ml) alone or together with 10 μM butyrate. After coculture with B1 cells from young mice for 2 days, only monocytes treated with LPS, but not LPS plus butyrate, readily converted 4BL cells (fig. S7I). To validate this result in humans, we similarly stimulated peripheral blood monocytes from young human donors [which cannot induce 4BL cells (19, 20)] with saline, LPS, or LPS and butyrate. As seen in mice, only monocytes stimulated with LPS, but not LPS with butyrate nor saline treatment, up-regulated 4–1BBL in B cells (fig. S7J). Conversely, we replenished butyrate in aged mice by oral gavage for 20 days. The increased presence of monocytes, 4BL cells, and GrB$^+$CD8$^+$ T cells in aged mice was abolished in butyrate-treated aged mice (Fig. 5, C to E). We repeated the experiment with a new group of young, aged, and butyrate-treated aged mice. Two days after cessation of butyrate treatment, mice were intravenously injected with GFP$^+$ B1 cells from young mice. Consistent with the loss of host monocytes (Fig. 5C and fig. S8A), butyrate treatment in aged mice abolished the conversion of GFP$^+$ B1 cells into 4BL cells (Fig. 5, F and G, and fig. S8B). Together, we conclude that the butyrate reduction in aged mice, at least in part, allows microbial inflammatory stimuli to activate monocytes and thus induce 4BL cells.

4BL cells promote IR in aging

Because 4BL cells express 4–1BBL and TNFα [Fig. 1, J and K, and (19, 20)], which are implicated in obesity-induced adipose inflammation and metabolic disorders (21), we tested whether 4BL cells cause IR in aging (1). By measuring fasting plasma insulin and performing insulin tolerance test (ITT) and oral glucose tolerance test (OGTT), we confirmed that IR was increased in healthy aged mice compared to young mice (n = 38 to 46 mice per group; Fig. 6, A to C, and table S2). Compared to young mice, injection of insulin less efficiently induced Tyr phosphorylation (pTyr) of liver insulin receptor in aged mice (Fig. 6D). However, there was no difference in Akt activation between the two groups, suggesting that inhibition of insulin receptor signaling involves TNFα (39), which can be provided by 4BL cells. We therefore repeated experiments that reverse gut leakiness and eliminate 4BL cells in aged mice. Enrofloxacin treatment completely abolished the increased IR in aged mice (Fig. 6, E and F) presumably without affecting food intake, as the body weight of mice was not changed (fig. S8C). Similarly, when we treated aged mice with butyrate, the previously increased IR reverted to concentrations observed in young mice

(Fig. 6G). We also depleted $CD20^+$ B cells/4BL cells or their inducers, $CCR2^+$ monocytes, in aged mice by a 20-day treatment with 5D2 Ab (αCD20) and MC21 Ab (αCCR2), respectively. Unlike isotype control Ab treatment, the depletion of B cells/4BL cells or $CCR2^+$ monocytes (Fig. 2, D and E) completely abolished IR in the aged mice (Fig. 7, A to C). Because IR in obesity is also linked to $CD8^+$ T cells and neutrophils (40, 41), we tested whether they are required for aging IR. Depletion of these two cell types using αCD8 and αLy6G Abs did not improve insulin sensitivity nor insulin production in aged mice (fig. S8D). We wondered whether IR in aging might instead be mediated by 4BL cells. To test this possibility, we used B cell–deficient JHT mice that were fed for 4 months with a high-fat diet (HFD) to metabolically sensitize them without inducing IR (42). Mice were then intravenously transferred with congenic B1a cells from young mice or B1a (4BL) cells from aged mice. After 7 days, the IR was only up-regulated in mice replenished with 4BL cells, but not with young B1a cells (Fig. 7D). To further underscore the importance of 4BL cells, we repeated the Akk experiment in aged mice and found that, consistent with the above-noted depletion of 4BL cells, Akk abolished the increased IR and improved liver insulin signaling (Fig. 7, E to G) without changing fasting plasma insulin (fig. S8E). We repeated the Akk experiment and then intravenously transferred the mice with 4BL cells from wild-type (WT) or 4–1BBL knockout (KO) aged mice. The reintroduction of WT 4BL cells abolished the Akk- induced IR benefit, such as the reduced fasting plasma ITT and OGTT and the improved liver insulin receptor signaling (Fig. 7, E to G). In contrast, the transfer of 4–1BBL KO 4BL cells failed to increase IR (Fig. 7, E to G), implying that IR in aged mice is induced by 4BL cells and requires 4–1BBL.

To extrapolate these results to aged primates, we measured IR in young and mock- or enrofloxacin-treated elderly macaques ($n = 6$ per group). Compared with young primates, IR was increased in elderly macaques (Fig. 7H and fig. S8F). However, a 2-month enrofloxacin treatment, together with the above-noted loss of 4BL cells (Fig. 3, H and I), was sufficient to reverse IR (Fig. 7H and fig. S8F) almost back to the concentrations seen in young macaques.

DISCUSSION

Here, we report that gut commensal bacteria controls IR in healthy aging via inflammation and subsequent induction of 4BL cells. Our modeling studies with aged mice and macaques indicate that this process is triggered by the reduction of potentially protective bacteria and enrichment of pathogenic gut commensals from the Firmicutes phylum. We observed a decrease of beneficial *A. muciniphila* and members of SCFA producers of *Clostridium* clusters *IV* and *XIVa*, such as *I. butyriciproducens*, *F. prausnitzii*, *R. faecis*, and *A. butyraticus* (31, 32) in aged mice regardless of the vendor source. It is difficult to identify a single microbe that triggers inflammation, presumably due to potential functional redundancies and complex relationships between commensals and differences in diet and host species. However, the loss of *A. muciniphila* appears to be a key factor that initiates the monocyte–4BL cell–IR axis in aged SPF mice. *A. muciniphila* protects the intestinal integrity by activating epithelial cells, inducing production of mucus (12, 30), and thereby supporting growth of other beneficial commensals (30, 37), such as SCFA producers (43). This explains why replenishment with *A. muciniphila* alone or treatment with enrofloxacin, which increases its abundance, was sufficient to restore the mucus layer and block gut

leakiness, thereby abolishing the accumulation of 4BL cells and subsequently IR. By providing fermented mucus, *A. muciniphila* also stimulates intestinal butyrate production from butyrate-producing bacteria such as *F. prausnitzii* (44). Thus, the loss of *A. muciniphila* may have not only caused the above-noted reduction of SCFA producers but may also be directly responsible for the marked reduction of intestinal SCFAs, particularly butyrate, in aged mice and macaques. Because butyrate supports the intestinal epithelial integrity both by providing energy to other commensals and colonocytes (7) and by inhibiting the expansion of potentially proinflammatory and pathogenic commensals (8), its reduction in aging intestine is expected to further exacerbate the gut leakiness induced by the loss of *A. muciniphila*.

We showed that intestinal leakage, possibly of pathogenic commensals (perhaps Firmicutes) and their products such as LPS and palmitic acid (2), triggers a chain of inflammatory events that activate monocytes to convert B1a cells into 4BL cells in the omentum. Consistent with the increase of CCL2 and CXCL13 chemokines in frail elderly mice and humans (27, 45), their up-regulation in the inflamed PeC of aged mice may have caused corecruitment of $CCR2^+$ monocytes and $CXCR5^+$ B1a cells in the omentum. The intestinal leakage also activated $CCR2^+$ monocytes to up-regulate 4–1BB, CD40L, and IFN-γ, which we previously reported to be essential in 4BL cell conversion, as they trigger 4–1BBL, CD40, and IFN-γR1 signaling in B1a cells (19, 20). Although aging PeC was enriched in dendritic cells, they appear to be a minor player in the 4BL cell conversion. Similarly, resident macrophages did not induce the conversion, consistent with the aging-associated decrease of their numbers and phagocytic function (46). Instead, we link the 4BL cell induction to $CCR2^+Ly6C^{hi}$ monocytes and possibly their early/intermediate macrophage subsets differentiated in the inflamed milieu (22). However, $CCR2^+Ly6C^{hi}$ monocyte activation and thus 4BL cell conversion were controlled by butyrate, a potent inhibitor of TLR4 signaling in myeloid cells (38). Our results suggest that the butyrate decrease in the gut and PeC of aged hosts enables LPS and other microbial stimuli to activate $CCR2^+$ monocytes to subsequently induce 4BL cells and thereby IR. Thus, the conversion of 4BL cells can be induced or blocked by changing the butyrate/microbial stimuli ratio, such as by in vitro and in vivo treatment of monocytes or young mice with LPS or LPS + butyrate, or by supplementing aged mice with butyrate.

Overall, as summarized in fig. S9, our results underscore the importance of gut microbiota in “healthy” aging. Consistent with a positive association between leaky gut and various autoimmune and metabolic diseases (47), we found evidence that loss of *A. muciniphila* in aging impairs the intestinal integrity and increases gut leakiness that triggers a chain of events that culminate in IR. The *A. muciniphila* loss may lead to the decrease in other commensals, such *I. butyriciproducens*, *F. prausnitzii*, *R. faecis*, and *A. butyraticus*, and thus their beneficial metabolites, particularly butyrate. When gut is leaky, the reduction of this important inhibitor of TLR4 signaling (38) in PeC enables endotoxin and other bacterial products to freely activate $CCR2^+$ monocyte up-regulating 4–1BB, CD40L, and IFN-γ. Upon coinfiltration into inflamed aging omentum, activated $CCR2^+$ monocyte convert B1a cells into 4BL cells. Then, 4BL cells induce IR in a 4–1BBL–dependent manner in aged mice without affecting production of insulin. However, this pathway is reversible in both aged mice and macaques. It can be blocked by strategies that reverse gut leakiness, such as

enrofloxacin treatment (and possibly by other Abx that increase *Akkermansia*), by replenishing *A. muciniphila* or butyrate, or by inactivating their downstream target cells, monocytes, or 4BL cells. As in our aged mice, where IR requires expression of 4–1BBL in 4BL cells, the 4–1BBL receptor 4–1BB and TNFα signaling have been implicated in glucose tolerance and IR in HFD-fed mice (21). Moreover, *A. muciniphila* is reported to be among the most reduced commensals in mice with diet-induced obesity and humans with type 2 diabetes (T2D) (2, 35). This may explain why IR and diet-induced obesity in mice associate with decreased concentrations of butyrate (12, 48–50) and increased gut leakage of commensals and endotoxemia (51, 52) and, conversely, why these pathologies benefit from the presence of *A. muciniphila* and butyrate (12, 49, 50). Therefore, it is tempting to speculate whether metabolic disorder and IR in diet-induced obesity are also mediated by 4BL cells. Although IR in aged mice was not affected by the depletion of $CD8^+$ T cells, it remains to be seen whether the effects of $CD8^+$ T cells and neutrophils on diet-induced IR in mice (40, 41) are due to the ability of 4BL cells to induce GrB^+CD8^+ T cells (19, 20) or their potential cross-talk with myeloid cells. Recently, the use of B1a cells was proposed as a strategy to ameliorate T2D in diet-induced obesity (53). In cases of increased gut leakiness or where *A. muciniphila* and butyrate are reduced (54), we think that this strategy may only provide a transient benefit or may even be harmful. As we have shown here and elsewhere (20), and consistent with the implications of 4–1BB and TNFα in obesity-induced T2D (21), B1a cells up-regulate 4–1BBL and mTNFα to become pathogenic 4BL cells within a few days after transfer into aged mice. Thus, besides their loss of immunosuppressive ability and acquisition of the ability to induce cytolytic GrB^+CD8^+ T cells capable of killing tumors (19, 20), these cells may promote IR as in our aged mice and macaques. Because elderly humans accumulate 4BL cells (19, 20), which can be induced by LPS-stimulated monocytes, we conclude that their microbiota–monocyte–4BL cell axis may also be responsible for induction of IR as in aged mice and macaques. In concordance, the gut microbiota of the elderly, particularly when they are frail, contains proinflammatory *Bacteroidetes*-predominated commensals (5). Moreover, *A. muciniphila* also inversely associates with the human prediabetic state (55), which, together with beneficial SCFAs and polyamines, is markedly reduced in elderly frail people (4, 5, 56, 57), implying that the IR and other pathologies associated with aging and even frailty can be ameliorated by targeting the microbiota–monocyte–4BL cell axis.

MATERIALS AND METHODS

Study design

To search for links between IR and accumulation of potentially pathogenic 4BL cells, we used young (10 to 12 weeks) and aged (18 to 24 months) female C57BL/6 mice ($n = 400$), rhesus monkeys (*Macaca mulatta*, $n = 19$), and squirrel monkeys (*Saimiri sciureus*, $n = 9$). Experiments were conducted under the Guide for the Care and Use of Laboratory Animals (National Institutes of Health Publication No. 86–23, 1985). To evaluate the importance of the gut microbiome in the activation of 4BL cells, mice and macaques were treated with enrofloxacin (Abx, $n = 6$ to 12) for 3 to 4 months. We also sequenced the 16*S* rRNA genes of fecal microbes and quantified SCFAs in various regions of the intestine and in the PeC of untreated or Abx-treated young and aged mice. To link the induction of 4BL cells to

microbiome-induced monocytes, we used oral fecal transplantation and gavaged young germ-free or aged SPF mice with cultured Akk. To link 4BL cells to IR induction, mice were adoptively transferred with 4BL cells from WT or 4–1BBL KO aged mice. In addition, aged mice were depleted of 4BL cells or monocytes using respective Abs. Experimental and control groups were age-matched for all studies. Details on experimental replicates are provided in the relevant figure legends.

Statistical analysis

Results are presented as the means ± SEM. Sample size was 5 to 12 animals per group, randomized by age (19, 20). For primates, we used all available rhesus monkeys (*M. mulatta*, $n = 19$) and squirrel monkeys (*S. sciureus*, $n = 9$); no animals were excluded in the analysis. Experiments were run in a blinded manner although outcome assessment was not blinded. GraphPad Prism (Prism 6; Graph Pad Software Inc.) was used to perform statistical analysis. For pairwise comparisons, a nonparametric paired Mann-Whitney U test was used. For three or more matched groups, a Kruskal-Wallis test with Dunn's correction was used. For the above tests, $*P < 0.05$, $**P < 0.01$, and $***P < 0.001$ throughout. For correlation studies, Spearman's correlation was used, and a P value less than 0.05 was considered statistically significant.

Supplementary Material

Refer to Web version on PubMed Central for supplementary material.

Acknowledgments:

We are grateful to A. Dzutsev and R. Winkler-Pickett (NCI) for running the NanoString assay; S. Ensor (Charles River Laboratories/NIA) for help with microbiota gavage experiments; J. W. Herzog (Division of Laboratory Animal Medicine, UNC at Chapel Hill) for providing germ-free mice; B. Wang (JRDUS) for help with fatty acid analysis; A. C. Chan (Genentech Inc.) for providing anti-CD20 Ab; S. Tajuddin (NIA/NIH) for help with statistical analysis; H. Hao (Johns Hopkins University Microarray Core), S. Sen, Y. Wuxing, V. Thovarai, and C. Ohuigin (NCI/NIH) for help with microbiota sequencing and analysis; and A. Lustig (NIA/NIH) and M. Deluca (U. Maryland, College Park, MD) for proofreading.

Funding: This research was supported by the Intramural Research Program of the National Institute on Aging, NIH (to A.B.); grants NIH RO1 DK103761 (to N.S.) and NIH R01 AG054712-01A1 and Russian Scientific Foundation grant 14-44-00077 (to E.R.); and CRADA with Janssen Research & Development, LLC (to A.B.).

REFERENCES AND NOTES

1. Fabbri E, Chia CW, Spencer RG, Fishbein KW, Reiter DA, Cameron D, Zane AC, Moore ZA, Gonzalez-Freire M, Zoli M, Studenski SA, Kalyani RR, Egan JM, Ferrucci L, Insulin resistance is associated with reduced mitochondrial oxidative capacity measured by ^{31}P-magnetic resonance spectroscopy in participants without diabetes from the baltimore longitudinal study of aging. Diabetes 66, 170–176 (2017). [PubMed: 27737951]
2. Mariat D, Firmesse O, Levenez F, Guimarães V, Sokol H, Doré J, Corthier G, Furet JP, The *Firmicutes/Bacteroidetes* ratio of the human microbiota changes with age. BMC Microbiol. 9, 123 (2009). [PubMed: 19508720]
3. Bauernfeind F, Niepmann S, Knolle PA, Hornung V, Aging-associated TNF production primes inflammasome activation and NLRP3-related metabolic disturbances. J. Immunol 197, 2900–2908 (2016). [PubMed: 27566828]

4. Biagi E, Nylund L, Candela M, Ostan R, Bucci L, Pini E, Nikkila J, Monti D, Satokari R, Franceschi C, Brigidi P, De Vos W, Through ageing, and beyond: Gut microbiota and inflammatory status in seniors and centenarians. PLOS ONE 5, e10667 (2010). [PubMed: 20498852]
5. Kong F, Hua Y, Zeng B, Ning R, Li Y, Zhao J, Gut microbiota signatures of longevity. Curr. Biol 26, R832–R833 (2016). [PubMed: 27676296]
6. Rampelli S, Candela M, Turroni S, Biagi E, Collino S, Franceschi C, O'Toole PW, Brigidi P, Functional metagenomic profiling of intestinal microbiome in extreme ageing. Aging 5, 902–912 (2013). [PubMed: 24334635]
7. Macia L, Tan J, Vieira AT, Leach K, Stanley D, Luong S, Maruya M, Ian McKenzie C, Hijikata A, Wong C, Binge L, Thorburn AN, Chevalier N, Ang C, Marino E, Robert R, Offermanns S, Teixeira MM, Moore RJ, Flavell RA, Fagarasan S, Mackay CR, Metabolite-sensing receptors GPR43 and GPR109A facilitate dietary fibre-induced gut homeostasis through regulation of the inflammasome. Nat. Commun 6, 6734 (2015). [PubMed: 25828455]
8. Byndloss MX, Olsan EE, Rivera-Chávez F, Tiffany CR, Cevallos SA, Lokken KL, Torres TP, Byndloss AJ, Faber F, Gao Y, Litvak Y, Lopez CA, Xu G, Napoli E, Giulivi C, Tsolis RM, Revzin A, Lebrilla CB, Bäumler AJ, Microbiota-activated PPAR-γ signaling inhibits dysbiotic Enterobacteriaceae expansion. Science 357, 570–575 (2017). [PubMed: 28798125]
9. Chang PV, Hao LM, Offermanns S, Medzhitov R, The microbial metabolite butyrate regulates intestinal macrophage function via histone deacetylase inhibition. Proc. Natl. Acad. Sci. U.S.A 111, 2247–2252 (2014). [PubMed: 24390544]
10. Furusawa Y, Obata Y, Fukuda S, Endo TA, Nakato G, Takahashi D, Nakanishi Y, Uetake C, Kato K, Kato T, Takahashi M, Fukuda NN, Murakami S, Miyauchi E, Hino S, Atarashi K, Onawa S, Fujimura Y, Lockett T, Clarke JM, Topping DL, Tomita M, Hori S, Ohara O, Morita T, Koseki H, Kikuchi J, Honda K, Hase K, Ohno H, Commensal microbe-derived butyrate induces the differentiation of colonic regulatory T cells. Nature 504, 446–450 (2013). [PubMed: 24226770]
11. Nastasi C, Candela M, Bonefeld CM, Geisler C, Hansen M, Krejsgaard T, Biagi E, Andersen MH, Brigidi P, Ødum N, Litman T, Woetmann A, The effect of short-chain fatty acids on human monocyte-derived dendritic cells. Sci. Rep 5, 16148 (2015). [PubMed: 26541096]
12. Plovier H, Everard A, Druart C, Depommier C, Van Hul M, Geurts L, Chilloux J, Ottman N, Duparc T, Lichtenstein L, Myridakis A, Delzenne NM, Klievink J, Bhattacharjee A, van der Ark KC, Aalvink S, Martinez LO, Dumas ME, Maiter D, Loumaye A, Hermans MP, Thissen JP, Belzer C, de Vos WM, Cani PD, A purified membrane protein from *Akkermansia muciniphila* or the pasteurized bacterium improves metabolism in obese and diabetic mice. Nat. Med 23, 107–113 (2017). [PubMed: 27892954]
13. Hearps AC, Martin GE, Angelovich TA, Cheng WJ, Maisa A, Landay AL, Jaworowski A, Crowe SM, Aging is associated with chronic innate immune activation and dysregulation of monocyte phenotype and function. Aging Cell 11, 867–875 (2012). [PubMed: 22708967]
14. Bouchlaka MN, Sckisel GD, Chen M, Mirsoian A, Zamora AE, Maverakis E, Wilkins DE, Alderson KL, Hsiao HH, Weiss JM, Monjazeb AM, Hesdorffer C, Ferrucci L, Longo DL, Blazar BR, Wiltrout RH, Redelman D, Taub DD, Murphy WJ, Aging predisposes to acute inflammatory induced pathology after tumor immunotherapy. J. Exp. Med 210, 2223–2237 (2013). [PubMed: 24081947]
15. Morrison SJ, Wandycz AM, Akashi K, Globerson A, Weissman IL, The aging of hematopoietic stem cells. Nat. Med 2, 1011–1016 (1996). [PubMed: 8782459]
16. Koch S, Larbi A, Derhovanessian E, Ozcelik D, Naumova E, Pawelec G, Multiparameter flow cytometric analysis of CD4 and CD8 T cell subsets in young and old people. Immun. Ageing 5, 6 (2008). [PubMed: 18657274]
17. Rubtsov AV, Rubtsova K, Fischer A, Meehan RT, Gillis JZ, Kappler JW, Marrack P, Toll-like receptor 7 (TLR7)-driven accumulation of a novel CD11c+ B-cell population is important for the development of autoimmunity. Blood 118, 1305–1315 (2011). [PubMed: 21543762]
18. Hao Y, O'Neill P, Naradikian MS, Scholz JL, Cancro MP, A B-cell subset uniquely responsive to innate stimuli accumulates in aged mice. Blood 118, 1294–1304 (2011). [PubMed: 21562046]
19. Lee-Chang C, Bodogai M, Moritoh K, Olkhanud PB, Chan AC, Croft M, Mattison JA, Holst PJ, Gress RE, Ferrucci L, Hakim F, Biragyn A, Accumulation of 4–1BBL^{+} B cells in the elderly

induces the generation of granzyme-B$^+$ CD8$^+$ T cells with potential antitumor activity. Blood 191, 1450–1459 (2014).

20. Lee-Chang C, Bodogai M, Moritoh K, Chen X, Wersto R, Sen R, Young HA, Croft M, Ferrucci L, Biragyn A, Aging converts innate B1a cells into potent CD8$^+$ T cell inducers. J. Immunol 196, 3385–3397 (2016). [PubMed: 26983789]
21. Kim CS, Kim JG, Lee BJ, Choi MS, Choi HS, Kawada T, Lee KU, Yu R, Deficiency for costimulatory receptor 4–1BB protects against obesity-induced inflammation and metabolic disorders. Diabetes 60, 3159–3168 (2011). [PubMed: 21998397]
22. Gordon S, Taylor PR, Monocyte and macrophage heterogeneity. Nat. Rev. Immunol 5, 953–964 (2005). [PubMed: 16322748]
23. Kanda H, Tateya S, Tamori Y, Kotani K, Hiasa K, Kitazawa R, Kitazawa S, Miyachi H, Maeda S, Egashira K, Kasuga M, MCP-1 contributes to macrophage infiltration into adipose tissue, insulin resistance, and hepatic steatosis in obesity. J. Clin. Invest 116, 1494–1505 (2006). [PubMed: 16691291]
24. Wols HA, Johnson KM, Ippolito JA, Birjandi SZ, Su Y, Le PT, Witte PL, Migration of immature and mature B cells in the aged microenvironment. Immunology 129, 278–290 (2010). [PubMed: 19845796]
25. Berberich S, Förster R, Pabst O, The peritoneal micromilieu commits B cells to home to body cavities and the small intestine. Blood 109, 4627–4634 (2007). [PubMed: 17289810]
26. Bassols J, Ortega FJ, Moreno-Navarrete JM, Peral B, Ricart W, Fernández-Real JM, Study of the proinflammatory role of human differentiated omental adipocytes. J. Cell. Biochem 107, 1107–1117 (2009). [PubMed: 19492335]
27. Rangel-Moreno J, Moyron-Quiroz JE, Carragher DM, Kusser K, Hartson L, Moquin A, Randall TD, Omental milky spots develop in the absence of lymphoid tissue-inducer cells and support B and T cell responses to peritoneal antigens. Immunity 30, 731–743 (2009). [PubMed: 19427241]
28. Mildner A, Mack M, Schmidt H, Brück W, Djukic M, Zabel MD, Hille A, Priller J, Prinz M, CCR2$^+$Ly-6Chi monocytes are crucial for the effector phase of autoimmunity in the central nervous system. Brain 132, 2487–2500 (2009). [PubMed: 19531531]
29. Chassaing B, Srinivasan G, Delgado MA, Young AN, Gewirtz AT, Vijay-Kumar M, Fecal lipocalin 2, a sensitive and broadly dynamic non-invasive biomarker for intestinal inflammation. PLOS ONE 7, e44328 (2012). [PubMed: 22957064]
30. Derrien M, Belzer C, de Vos WM, *Akkermansia muciniphila* and its role in regulating host functions. Microb. Pathog 106, 171–181 (2017). [PubMed: 26875998]
31. Barcenilla A, Pryde SE, Martin JC, Duncan SH, Stewart CS, Henderson C, Flint HJ, Phylogenetic relationships of butyrate-producing bacteria from the human gut. Appl. Environ. Microb 66, 1654–1661 (2000).
32. Eeckhaut V, Van Immerseel F, Pasmans F, De Brandt E, Haesebrouck F, Ducatelle R, Vandamme P, Anaerostipes butyraticus sp. nov., an anaerobic, butyrate-producing bacterium from Clostridium cluster XIVa isolated from broiler chicken caecal content, and emended description of the genus Anaerostipes. Int. J. Syst. Evol. Microbiol 60, 1108–1112 (2010). [PubMed: 19666785]
33. Kläring K, Hanske L, Bui N, Charrier C, Blaut M, Haller D, Plugge CM, Clavel T, *Intestinimonas butyriciproducens* gen. nov., sp. nov., a butyrate-producing bacterium from the mouse intestine. Int. J. Syst. Evol. Microbiol 63, 4606–4612 (2013). [PubMed: 23918795]
34. Everard A, Belzer C, Geurts L, Ouwerkerk JP, Druart C, Bindels LB, Guiot Y, Derrien M, Muccioli GG, Delzenne NM, de Vos WM, Cani PD, Cross-talk between *Akkermansia muciniphila* and intestinal epithelium controls diet-induced obesity. Proc. Natl. Acad. Sci. U.S.A 110, 9066–9071 (2013). [PubMed: 23671105]
35. Thevaranjan N, Puchta A, Schulz C, Naidoo A, Szamosi JC, Verschoor CP, Loukov D, Schenck LP, Jury J, Foley KP, Schertzer JD, Larché MJ, Davidson DJ, Verdú EF, Surette MG, Bowdish DME, Age-associated microbial dysbiosis promotes intestinal permeability, systemic inflammation, and macrophage dysfunction. Cell Host Microbe 21, 455–466.e4 (2017). [PubMed: 28407483]
36. Dubourg G, Lagier JC, Armougom F, Robert C, Audoly G, Papazian L, Raoult D, High-level colonisation of the human gut by Verrucomicrobia following broad-spectrum antibiotic treatment. Int. J. Antimicrob. Agents 41, 149–155 (2013). [PubMed: 23294932]

37. Finnie IA, Dwarakanath AD, Taylor BA, Rhodes JM, Colonic mucin synthesis is increased by sodium butyrate. Gut 36, 93–99 (1995). [PubMed: 7890244]
38. Cox MA, Jackson J, Stanton M, Rojas-Triana A, Bober L, Laverty M, Yang X, Zhu F, Liu J, Wang S, Monsma F, Vassileva G, Maguire M, Gustafson E, Bayne M, Chou CC, Lundell D, Jenh CH, Short-chain fatty acids act as antiinflammatory mediators by regulating prostaglandin E_2 and cytokines. World J. Gastroenterol 15, 5549–5557 (2009). [PubMed: 19938193]
39. Ozes ON, Akca H, Mayo LD, Gustin JA, Maehama T, Dixon JE, Donner DB, A phosphatidylinositol 3-kinase/Akt/mTOR pathway mediates and PTEN antagonizes tumor necrosis factor inhibition of insulin signaling through insulin receptor substrate-1. Proc. Natl. Acad. Sci. U.S.A 98, 4640–4645 (2001). [PubMed: 11287630]
40. Nishimura S, Manabe I, Nagasaki M, Eto K, Yamashita H, Ohsugi M, Otsu M, Hara K, Ueki K, Sugiura S, Yoshimura K, Kadowaki T, Nagai R, $CD8^+$ effector T cells contribute to macrophage recruitment and adipose tissue inflammation in obesity. Nat. Med 15, 914–920 (2009). [PubMed: 19633658]
41. Talukdar S, Oh DY, Bandyopadhyay G, Li D, Xu J, McNelis J, Lu M, Li P, Yan Q, Zhu Y, Ofrecio J, Lin M, Brenner MB, Olefsky JM, Neutrophils mediate insulin resistance in mice fed a high-fat diet through secreted elastase. Nat. Med 18, 1407–1412 (2012). [PubMed: 22863787]
42. Winer DA, Winer S, Shen L, Wadia PP, Yantha J, Paltser G, Tsui H, Wu P, Davidson MG, Alonso MN, Leong HX, Glassford A, Caimol M, Kenkel JA, Tedder TF, McLaughlin T, Miklos DB, Dosch H-M, Engleman EG, B cells promote insulin resistance through modulation of T cells and production of pathogenic IgG antibodies. Nat. Med 17, 610–617 (2011). [PubMed: 21499269]
43. Nava GM, Friedrichsen HJ, Stappenbeck TS, Spatial organization of intestinal microbiota in the mouse ascending colon. ISME J. 5, 627–638 (2011). [PubMed: 20981114]
44. Belzer C, Chia LW, Aalvink S, Chamlagain B, Piironen V, Knol J, de Vos WM, Microbial metabolic networks at the mucus layer lead to diet-independent butyrate and vitamin B12 production by intestinal symbionts. MBio 8, e00770–17 (2017). [PubMed: 28928206]
45. Yousefzadeh MJ, Schafer MJ, Noren Hooten N, Atkinson EJ, Evans MK, Baker DJ, Quarles EK, Robbins PD, Ladiges WC, LeBrasseur NK, Niedernhofer LJ, Circulating levels of monocyte chemoattractant protein-1 as a potential measure of biological age in mice and frailty in humans. Aging Cell 17, e12706 (2017).
46. Linehan E, Dombrowski Y, Snoddy R, Fallon PG, Kissenpfennig A, Fitzgerald DC, Aging impairs peritoneal but not bone marrow-derived macrophage phagocytosis. Aging Cell 13, 699–708 (2014). [PubMed: 24813244]
47. Mu Q, Kirby J, Reilly CM, Luo XM, Leaky gut as a danger signal for autoimmune diseases. Front. Immunol 8, 598 (2017). [PubMed: 28588585]
48. Schneeberger M, Everard A, Gómez-Valadés AG, Matamoros S, Ramírez S, Delzenne NM, Gomis R, Claret M, Cani PD, Akkermansia muciniphila inversely correlates with the onset of inflammation, altered adipose tissue metabolism and metabolic disorders during obesity in mice. Sci. Rep 5, 16643 (2015). [PubMed: 26563823]
49. Greer RL, Dong X, Moraes ACF, Zielke RA, Fernandes GR, Peremyslova E, Vasquez-Perez S, Schoenborn AA, Gomes EP, Pereira AC, Ferreira SRG, Yao M, Fuss IJ, Strober W, Sikora AE, Taylor GA, Gulati AS, Morgun A, Shulzhenko N, *Akkermansia muciniphila* mediates negative effects of IFNγ on glucose metabolism. Nat. Commun 7, 13329 (2016). [PubMed: 27841267]
50. Gao Z, Yin J, Zhang J, Ward RE, Martin RJ, Lefevre M, Cefalu WT, Ye J, Butyrate improves insulin sensitivity and increases energy expenditure in mice. Diabetes 58, 1509–1517 (2009). [PubMed: 19366864]
51. Ley RE, Bäckhed F, Turnbaugh P, Lozupone CA, Knight RD, Gordon JI, Obesity alters gut microbial ecology. Proc. Natl. Acad. Sci. U.S.A 102, 11070–11075 (2005). [PubMed: 16033867]
52. Caesar R, Reigstad CS, Bäckhed HK, Reinhardt C, Ketonen M, Lundén GÖ, Cani PD, Bäckhed F, Gut-derived lipopolysaccharide augments adipose macrophage accumulation but is not essential for impaired glucose or insulin tolerance in mice. Gut 61, 1701–1707 (2012). [PubMed: 22535377]
53. Shen L, Chng MHY, Alonso MN, Yuan R, Winer DA, Engleman EG, B-1a lymphocytes attenuate insulin resistance. Diabetes 64, 593–603 (2015). [PubMed: 25249575]

54. Tilg H, Moschen AR, Microbiota and diabetes: An evolving relationship. Gut 63, 1513–1521 (2014). [PubMed: 24833634]
55. Zhang X, Shen D, Fang Z, Jie Z, Qiu X, Zhang C, Chen Y, Ji L, Human gut microbiota changes reveal the progression of glucose intolerance. PLOS ONE 8, e71108 (2013). [PubMed: 24013136]
56. Matsumoto M, Kurihara S, Kibe R, Ashida H, Benno Y, Longevity in mice is promoted by probiotic-induced suppression of colonic senescence dependent on upregulation of gut bacterial polyamine production. PLOS ONE 6, e23652 (2011). [PubMed: 21858192]
57. Claesson MJ, Jeffery IB, Conde S, Power SE, O'Connor EM, Cusack S, Harris HMB, Coakley M, Lakshminarayanan B, O'Sullivan O, Fitzgerald GF, Deane J, O'Connor M, Harnedy N, O'Connor K, O'Mahony D, van Sinderen D, Wallace M, Brennan L, Stanton C, Marchesi JR, Fitzgerald AP, Shanahan F, Hill C, Ross RP, O'Toole PW, Gut microbiota composition correlates with diet and health in the elderly. Nature 488, 178–184 (2012). [PubMed: 22797518]
58. Zhao Y, Croft M, Dispensable role for 4–1BB and 4–1BBL in development of vaccinia virus-specific CD8 T cells. Immunol. Lett 141, 220–226 (2012). [PubMed: 22037570]
59. Park SW, Herrema H, Salazar M, Cakir I, Cabi S, Basibuyuk Sahin F, Chiu Y-H, Cantley LC, Ozcan U, BRD7 regulates XBP1s' activity and glucose homeostasis through its interaction with the regulatory subunits of PI3K. Cell Metab. 20, 73–84 (2014). [PubMed: 24836559]
60. Gupta J, del Barco Barrantes I, Igea A, Sakellariou SP, Pateras IS, Gorgoulis VG, Nebreda AR, Dual function of p38α MAPK in colon cancer: Suppression of colitis-associated tumor initiation but requirement for cancer cell survival. Cancer Cell 25, 484–500 (2014). [PubMed: 24684847]
61. Caporaso JG, Bittinger K, Bushman FD, DeSantis TZ, Andersen GL, Knight R, PyNAST: A flexible tool for aligning sequences to a template alignment. Bioinformatics 26, 266–267 (2010). [PubMed: 19914921]
62. Magoč T, Salzberg SL, FLASH: Fast length adjustment of short reads to improve genome assemblies. Bioinformatics 27, 2957–2963 (2011). [PubMed: 21903629]
63. Bolger AM, Lohse M, Usadel B, Trimmomatic: A flexible trimmer for Illumina sequence data. Bioinformatics 30, 2114–2120 (2014). [PubMed: 24695404]
64. Langmead B, Salzberg SL, Fast gapped-read alignment with Bowtie 2. Nat. Methods 9, 357–359 (2012). [PubMed: 22388286]
65. McDonald D, Price MN, Goodrich J, Nawrocki EP, DeSantis TZ, Probst A, Andersen GL, Knight R, Hugenholtz P, An improved Greengenes taxonomy with explicit ranks for ecological and evolutionary analyses of bacteria and archaea. ISME J. 6, 610–618 (2012). [PubMed: 22134646]
66. Wang Q, Garrity GM, Tiedje JM, Cole JR, Naive Bayesian classifier for rapid assignment of rRNA sequences into the new bacterial taxonomy. Appl. Environ. Microbiol 73, 5261–5267 (2007). [PubMed: 17586664]
67. Callahan BJ, Sankaran K, Fukuyama JA, McMurdie PJ, Holmes SP, Bioconductor Workflow for Microbiome Data Analysis: From raw reads to community analyses. F1000Res 5, 1492 (2016). [PubMed: 27508062]
68. McMurdie PJ, Holmes S, phyloseq: An R package for reproducible interactive analysis and graphics of microbiome census data. PLOS ONE 8, e61217 (2013). [PubMed: 23630581]
69. Cole JR, Wang Q, Fish JA, Chai B, McGarrell DM, Sun Y, Brown CT, Porras-Alfaro A, Kuske CR, Tiedje JM, Ribosomal Database Project: Data and tools for high throughput rRNA analysis. Nucleic Acids Res. 42, D633–D642 (2014). [PubMed: 24288368]
70. Quast C, Pruesse E, Yilmaz P, Gerken J, Schweer T, Yarza P, Peplies J, Glöckner FO, The SILVA ribosomal RNA gene database project: Improved data processing and web-based tools. Nucleic Acids Res. 41, D590–D596 (2013). [PubMed: 23193283]
71. Love MI, Huber W, Anders S, Moderated estimation of fold change and dispersion for RNA-seq data with DESeq2. Genome Biol. 15, 550 (2014). [PubMed: 25516281]
72. Benjamini Y, Drai D, Elmer G, Kafkafi N, Golani I, Controlling the false discovery rate in behavior genetics research. Behav. Brain Res 125, 279–284 (2001). [PubMed: 11682119]
73. Vaishnava S, Yamamoto M, Severson KM, Ruhn KA, Yu X, Koren O, Ley R, Wakeland EK, Hooper LV, The antibacterial lectin RegIIIγ promotes the spatial segregation of microbiota and host in the intestine. Science 334, 255–258 (2011). [PubMed: 21998396]

74. Han J, Lin KJ, Sequeira C, Borchers CH, An isotope-labeled chemical derivatization method for the quantitation of short-chain fatty acids in human feces by liquid chromatography-tandem mass spectrometry. Anal. Chim. Acta 854, 86–94 (2015). [PubMed: 25479871]

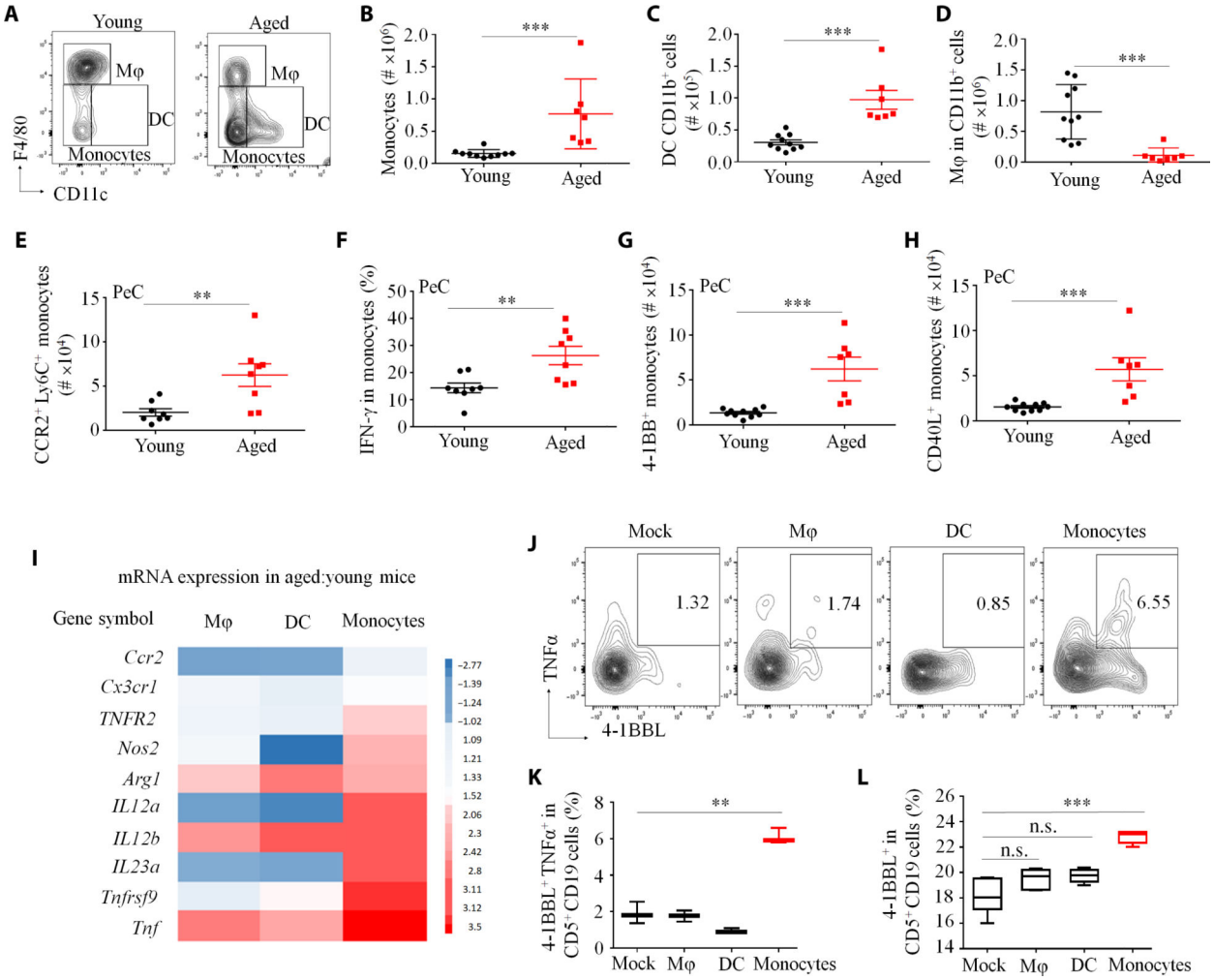

Fig. 1. Aging induces accumulation and activation of monocytes in the PeC.

(**A**) Shown is the gating strategy for myeloid cells (without granulocytes) in the PeC of young and aged mice. (**B** to **H**) Quantification of (B) monocytes, (C) dendritic cells (DC), (D) macrophages (Mφ), and (E) $CCR2^{+}Ly6C^{+}$ monocytes. (F to H) Aged mouse monocytes up-regulated key factors involved in 4BL cell conversion. *Y* axes show flow cytometry cell counts in individual mice ($n = 8$ to 10 per group, with each representative experiment reproduced at least three times). (**I**) *Z*-score heatmap of the change in the mRNA expression of selected genes in PeC Mφ, DC, and monocytes in aged compared to young mice ($n = 4$ per group; see also fig. S1, H and I). Only monocytes converted B1a cells into 4BL cells, as inferred by up-regulated surface expression of 4–1BBL and membrane (m) TNFα in $CD5^{+}CD19^{+}$ cells. (**J** to **L**) Sort-purified PeC Mφ, DC, and monocytes were cultured overnight with eFluor450-labeled B1 cells from young mice at a 1:1 ratio ($n = 4$ to 6 per group; the experiment was reproduced twice). Shown are representative flow cytometry data, with numbers showing the percentage of B1a cells expressing both 4–1BBL and TNFα ($n = 5$) (J) and its summary result for expression of 4–1BBL and TNFα in B1a cells (K and L). Data are represented as means ± SEM. $P < 0.05$, $^{**}P < 0.001$, and $^{***}P < 0.0001$ [Mann-

Whitney *U* test and Kruskal-Wallis test in (B) to (D), Dunn's test for multiple corrections in (K) and (L)]. n.s., not significant.

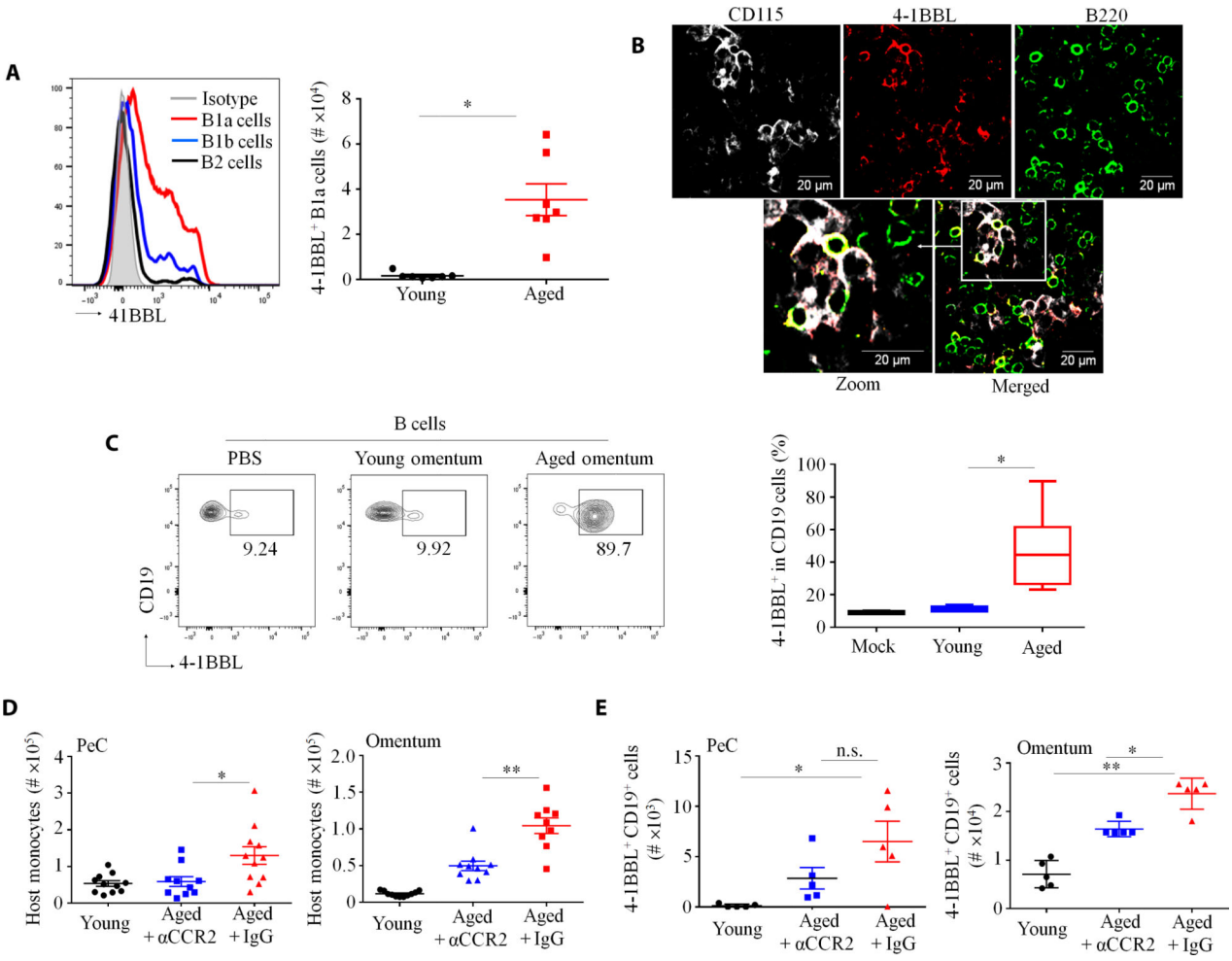

Fig. 2. CCR2$^+$ monocytes induce 4BL cell conversion in the omentum.

(**A**) B1a cells expressed more 4-BBL than B2 and B1b cells. Shown is a representative histogram for 4–1BBL expressing B cell types in aged omentum (left) and absolute numbers of 4–1BBL$^+$ B1a cells in the omentum of young and aged mice (right). Each symbol is for an independent mouse; $n = 7$ to 8 mice per group. (**B**) B220$^+$ (B cells) and 4–1BBL$^+$ cells colocalized with CD115$^+$ cells (monocytes) in a whole-mount immunofluorescence staining of aged omentum. (**C**) Compared to young omentum, aged mouse omentum efficiently converted eFluor450-labeled B1 cells from young mice into 4BL cells in vitro. Shown is a representative flow cytometric plot (left) and summary result (right) of B1 cells stimulated with phosphate-buffered saline (PBS), young omenta, or aged omenta ($n = 3$ mice per group; the experiment was reproduced twice). (**D** and **E**) The 4BL cell conversion was induced by CCR2$^+$ monocytes. After a 12-day treatment with control immunoglobulin G (IgG) or CCR2$^+$ monocyte–depleting Ab (αCCR2), aged mice were adoptively intravenously transferred with 5×10^6 GFP$^+$ B1 cells from young mice on day 13. Shown are (D) the number of host monocytes in PeC and omentum and (E) the number of donor GFP$^+$CD19$^+$ cells in PeC and omentum 4 days after B1 cell transfer ($n = 5$ mice per group; the experiment was reproduced three times). *$P < 0.05$ and **$P < 0.001$ (Kruskal-Wallis test with Dunn's test for multiple corrections in (C) to (E) and Mann-Whitney test for all others).

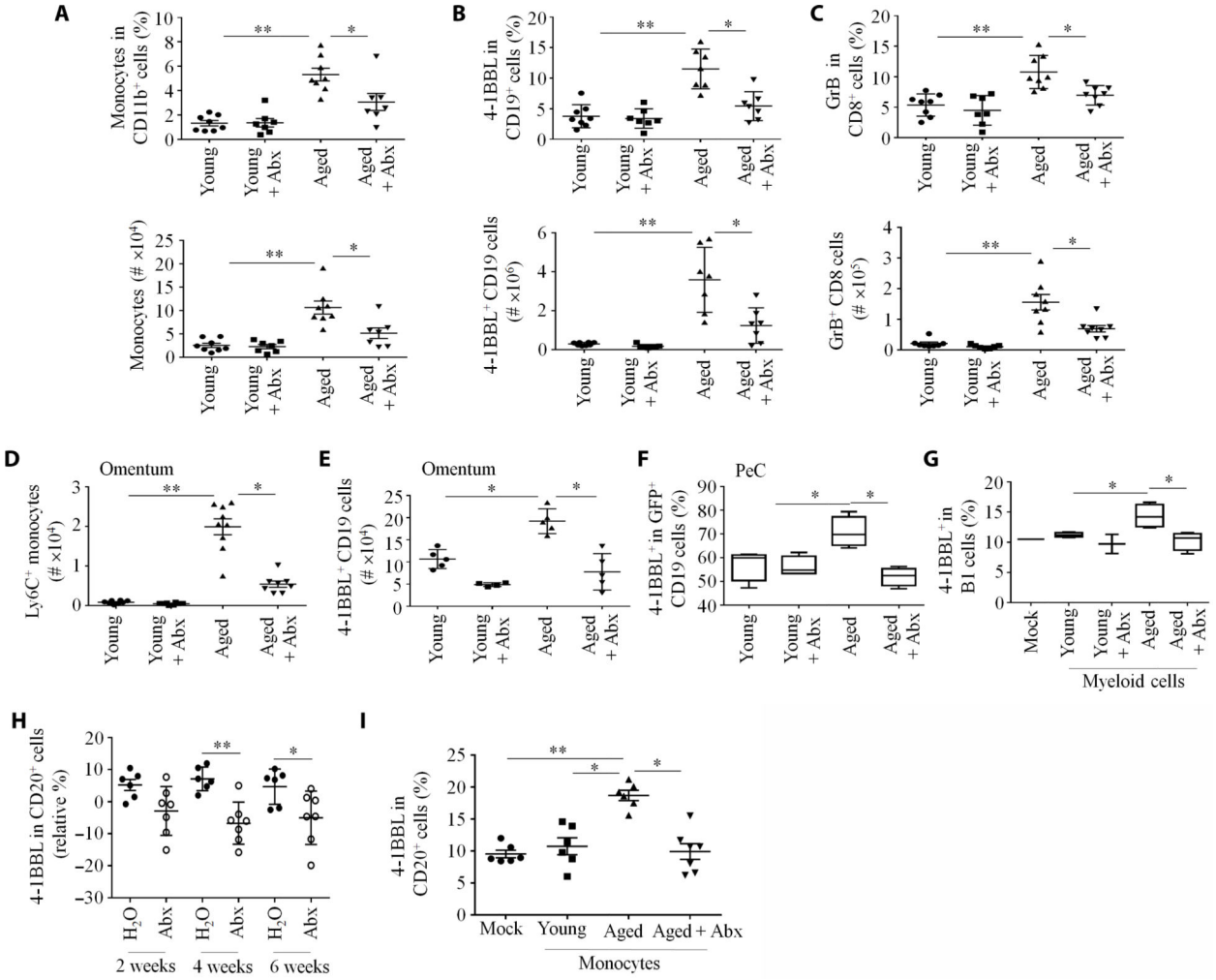

Fig. 3. Enrofloxacin (Abx) treatment eliminates the accumulation of monocytes and 4BL cells in aged mice.

(**A** to **G**) Young and aged mice (n = 7 to 9 per group) were treated with Abx (170 mg/liter) in drinking water for 3 to 4 months; representative results of experiments reproduced at least three times. The frequency (top) and absolute counts (bottom) of (A) monocytes, (B) 4BL cells, and (C) GrB^+CD8^+T cells in PeC were quantified. (D) and (E) show absolute counts of $Ly6C^+$ monocytes and 4BL cells, respectively, in the omentum of aged mice. (F) Abx-treated mice were intravenously injected with GFP^+ B1 cells from young mice to assess 4BL cell conversion in vivo after 5 days (n = 8 to 10 per group). (G) To evaluate the importance of monocytes in the 4BL cell conversion, flow-sorted PeC myeloid Lin^-CD11b^+ cells from mock- or Abx-treated young or aged mice were cultured overnight with $eFluor450^+$ PeC B cells from young mice at a 1:1 ratio (n = 6 to 8 per group). (**H**) Abx treatment decreased 4–1BBL $CD20^+$ B cells in the peripheral blood of elderly macaques (each symbol represents one individual; n = 6 to 7 per group). (**I**) Abx treatment impaired the monocyte-mediated 4BL cell conversion in macaques. $CD14^+$ monocytes from saline (mock)- or Abx-treated aged macaques were cultured overnight with $eFluor450^+$ $CD20^+$ cells from young macaques (n = 6 to 7 primates per group). *P < 0.05 and **P < 0.001 (Kruskal-Wallis test, Dunn's test for multiple corrections).

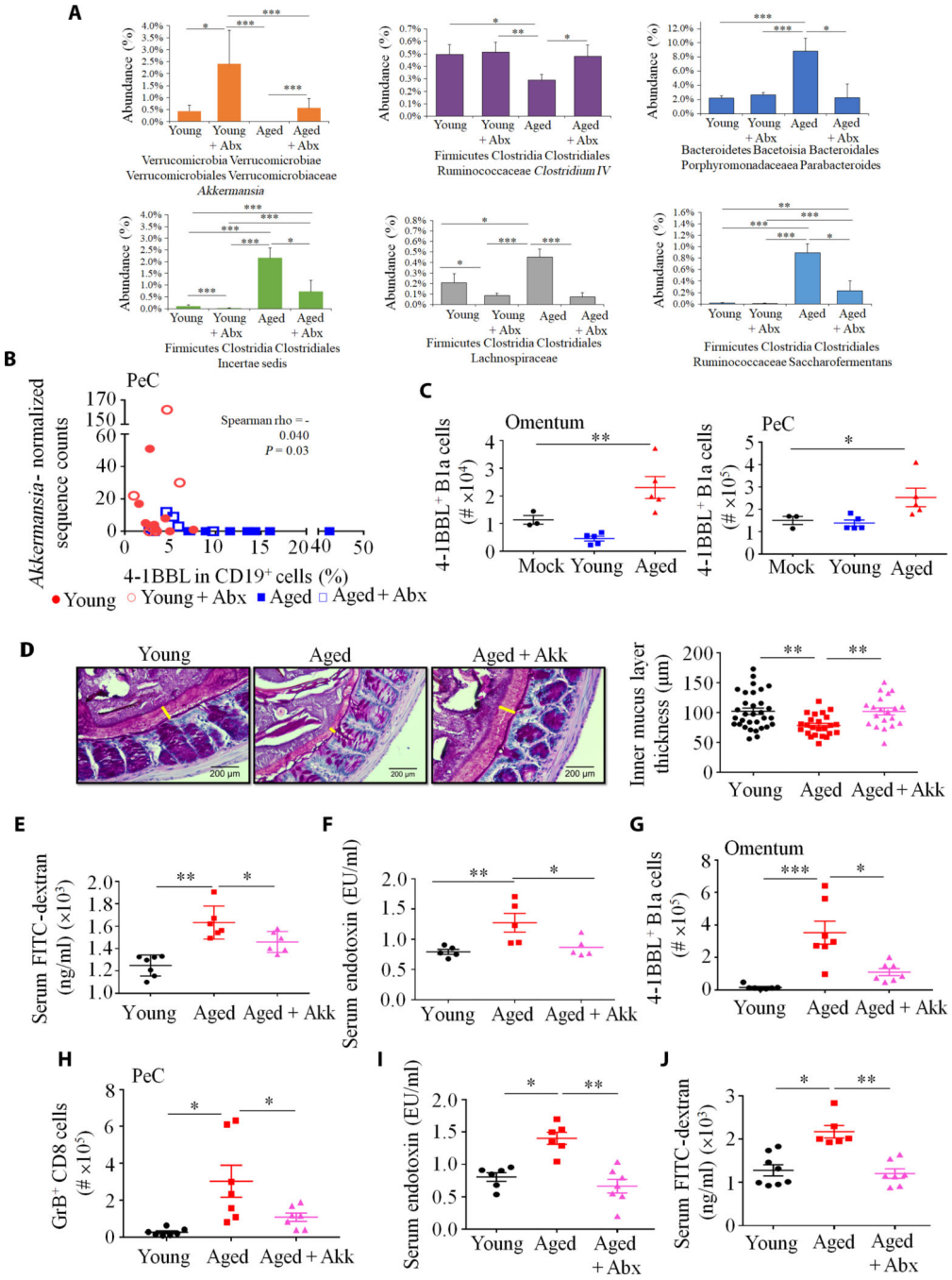

Fig. 4. Aging gut microbiota initiates the monocyte–4BL cell induction.

(**A**) The composition of gut microbiota was changed in aged mice. 16*S* rRNA gene sequencing results are shown as percent abundance of selected microbiota genera in murine feces ($n = 8$ mice per group). Note that *y*-axes lengths differ across plots. (**B**) *A. muciniphila* abundance inversely correlated with 4BL cells in PeC. Spearman correlations and associated *P* values are shown for each sample ($n = 7$ to 8 per group). (**C**) Gut microbiota of aged mice induced 4BL cells in 20-week-old germ-free mice. Shown are 4BL cells in the omentum and PeC of germ-free mice after weekly oral gavage with 25 µg of fecal suspension from SPF

aged or young mice for 4 weeks (n = 4 to 5 mice per group, experiment was reproduced three times). (**D**) A representative image (left) and quantification (right) show that the thickness of colonic inner mucus layer was reduced in aged mice, which was reversed after replenishment with *A. muciniphila* (1×10^8 colony-forming units, with oral gavage every second day for 20 days). The yellow bar indicates the inner mucus layer. (**E** and **F**) Aged mice showed increased gut permeability, which was restored by gavage with *A. muciniphila*, as shown by serum leakage of FITC-dextran (E) or endotoxin (F; n = 5 to 7 per group; the experiment was reproduced twice). The increase in 4BL cells (**G**) and their downstream GrB $^{+}$CD8^{+} T cells (**H**) in aged mice was not observed after *A. muciniphila* treatment (n = 6 to 8 per group; the experiment was reproduced three times). (**I**) Enrofloxacin (Abx) treatment (as in Fig. 3A) reversed gut permeability, as shown by serum endotoxin levels and (**J**) leakage of orally gavaged FITC-dextran (n = 8 per group). *P < 0.05, **P < 0.001, and ***P < 0.0001 (Kruskal-Wallis test with Dunn's test for multiple corrections). EU, endotoxin unit.

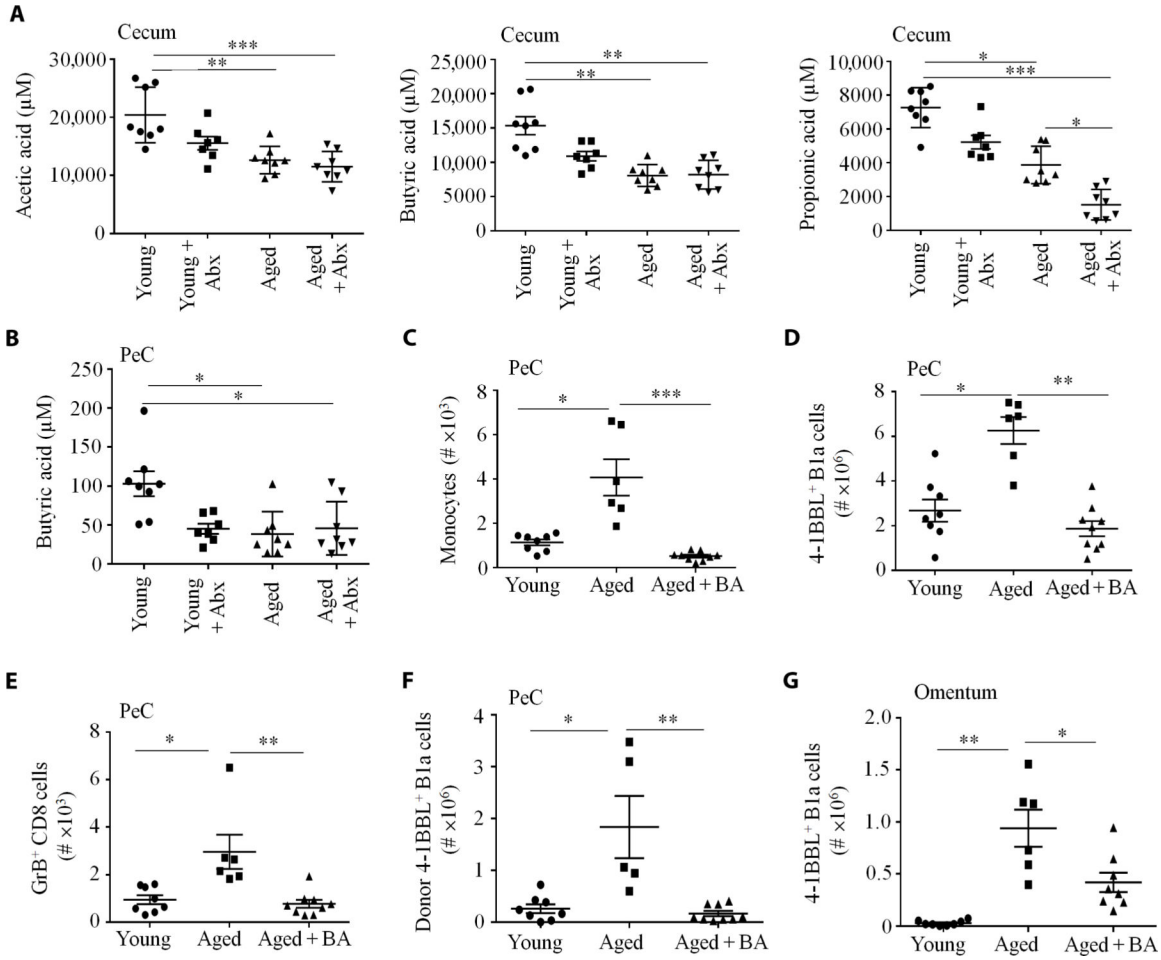

Fig. 5. The role of butyrate in 4BL conversion.

Compared to young mice, SCFAs (micromolar) in (**A**) cecum and (**B**) butyrate in PeC were markedly decreased in aged mice and after Abx treatment ($n = 7$ to 9 mice per group). Note that *y*-axes lengths differ across panels. Supplementation with butyrate (BA; oral gavage, 2.5 g/kg every second day for 4 weeks) decreased monocytes (**C**), 4BL cells (**D**), and GrB $^{+}$CD8^{+} T cells (**E**) in PeC ($n = 8$ per group; the experiment was reproduced twice). (**F** and **G**) Two days after the termination of BA [as in (C) to (E)], mice were intravenously transferred with PeC GFP^{+} B1 cells from young mice to evaluate their conversion into 4BL cells after 5 days in PeC (F) and omentum (G; $n = 6$ to 9 per group; the experiment was reproduced twice). Data are represented as means ± SEM. *$P < 0.05$, **$P < 0.001$, and ***$P < 0.0001$ (Mann-Whitney test and Kruskal-Wallis test with Dunn's test for multiple corrections).

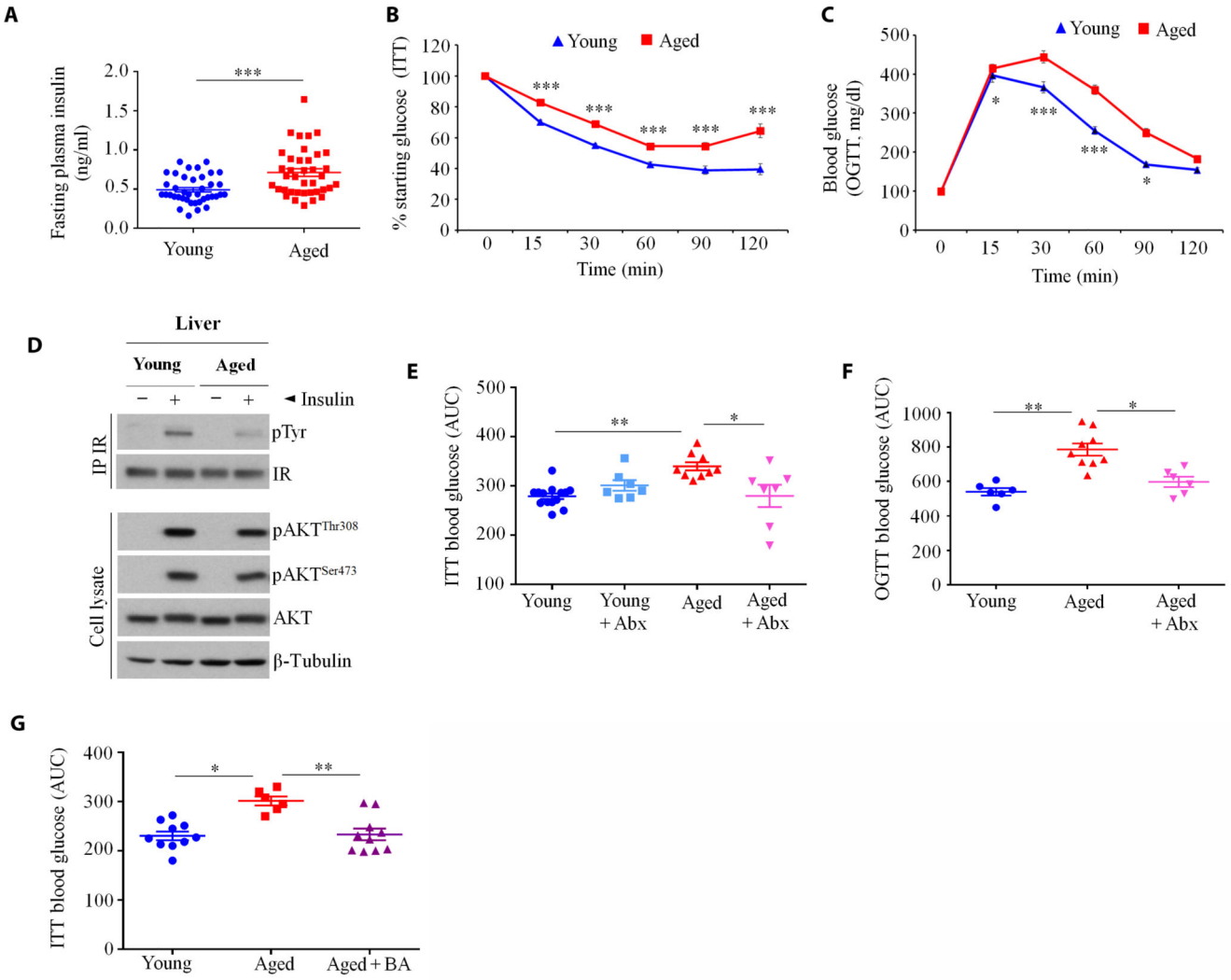

Fig. 6. IR is increased in aged mice.

(**A** to **C**) Measurements of (A) fasting plasma insulin concentrations (n = 38 to 46), (B) starting glucose in ITTs (n = 38 to 46), and (C) blood glucose concentrations in oral OGTTs (n = 38 to 46); each symbol indicates a single female C57BL/6 mouse. Plasma insulin levels were measured by enzyme-linked immunosorbent assay after overnight fasting. (**D**) Mice were injected with insulin, after which phosphorylation of the insulin receptor [pTyr, using immunoprecipitation (IP)] and AKT ($pThr^{308}$ and $pSer^{473}$) were quantified in liver lysates. (**E** to **G**) IR in aged mice is reversed by treatment with enrofloxacin (Abx), as measured by ITT (E) and OGTT (F; n = 7 to 9 per group, as in Fig. 3A) or (G) butyrate (BA; n = 8 to 10 per group, as in Fig. 5, C to G). *Y* axis in (E) to (G) shows area under the curve (AUC). Data are means ± SEM. *P < 0.05, **P < 0.001, and ***P < 0.0001 (Mann-Whitney test and Kruskal-Wallis test with Dunn's test for multiple corrections).

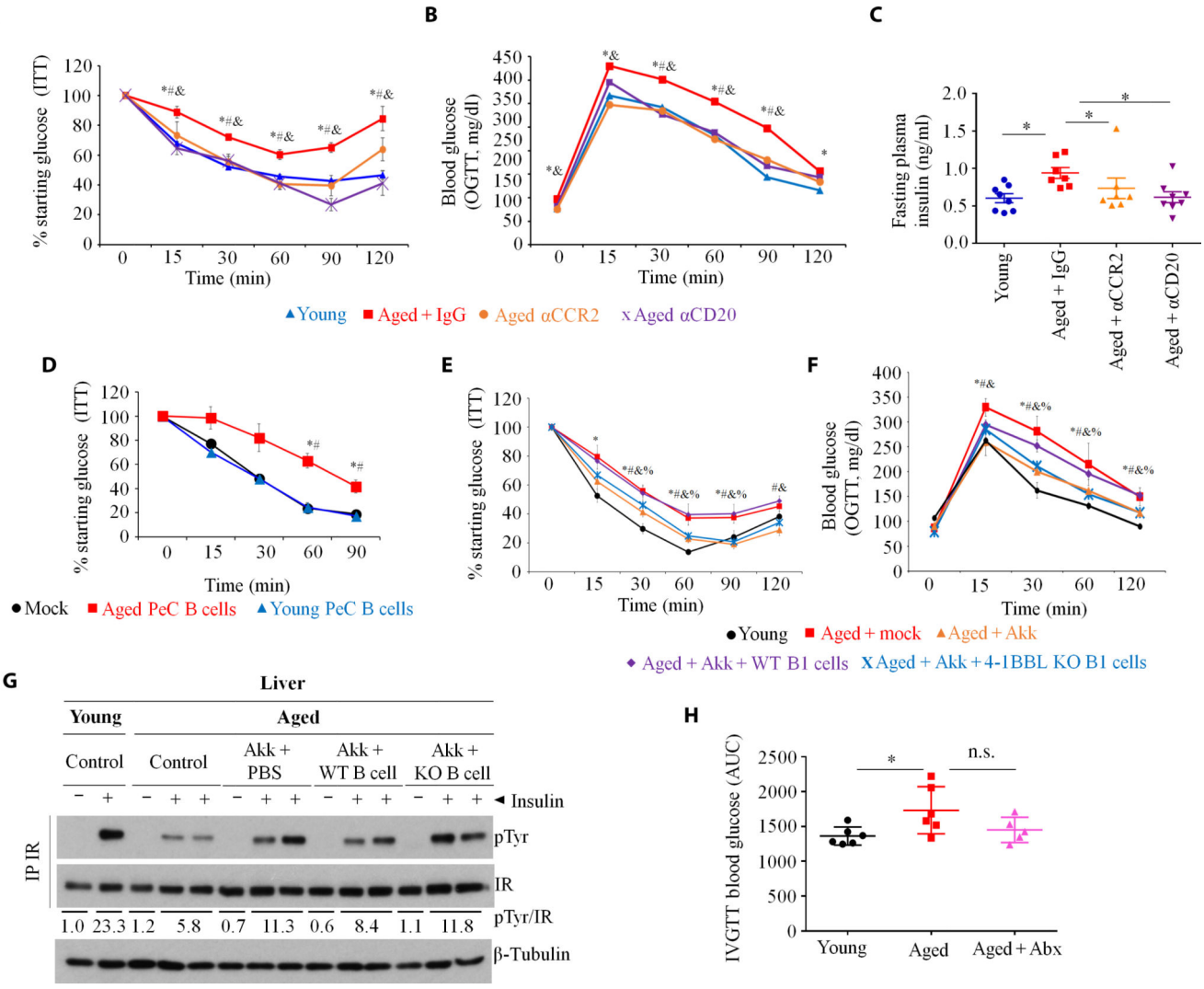

Fig. 7. Gut dysbiosis in aging promotes IR via 4BL cells.

(**A**) ITTs, (**B**) OGTTs, and (**C**) fasting plasma insulin show that IR in aged mice is reversed by the depletion of monocytes and B cells ($n = 7$ to 8 per group, as in Fig. 2D; "*," "#," and "&" show for $P < 0.05$ for comparisons of the following groups of mice: young versus aged + IgG, aged + IgG versus aged + αCCR2, or aged + αCD20, respectively). (**D**) Sort-purified or B1a cells from young or aged mice were intravenously transferred into B cell–deficient JHT mice fed with an HFD for 4 months. ITT was performed 1 week after intravenous transfer ($n = 10$ per group; "#" is for $P < 0.05$ for comparisons of PeC B cells from young versus aged mice). (**E** and **F**) Aged mice were gavaged with *A. muciniphila* for 20 days, but at day 14, mice were intravenously transferred with sort-purified B1a cells from the PeC of WT or 4–1BBL KO aged mice (Aged + Akk + WT B1 or Aged + Akk + KO B1, respectively) to evaluate IR at days 20 to 22 ($n = 8$ per group, with the experiment reproduced three times; "*," "#," "&," and "%" are for $P < 0.05$ for comparisons of the following groups of mice: young versus aged + mock, aged + mock versus aged + Akk, aged + Akk versus aged + Akk + WT B1, or aged + Akk + KO B1, respectively). (**G**) At day 24, mice in (E) and (F) were injected with insulin to quantify pTyr induction of the liver insulin

receptor (as in Fig. 6D). Numbers show the average pTyr increase normalized to β-tubulin. (**H**) IR was also increased in aged macaques (*M. mulatta*, $n = 6$ to 7 per group), which was reversed by Abx treatment (as in Fig. 3, H and I). Data are means ± SEM. $*P < 0.05$, $**P < 0.001$, and $***P < 0.0001$ (Mann-Whitney test and Kruskal-Wallis test with Dunn's test for multiple corrections).